COMSOL
CONFERENCE
2023 MUNICH

Understanding the Thermal Efficiency of Energy Quay Walls: A Comprehensive Study Using Field Tests and Finite Element Simulations

M. Gerola[1], F. Cecinato[1], J.K. Haasnoot[2], P.J. Vardon[3]
1. Dipartimento di Scienze della Terra "A. Desio", Università degli studi di Milano, Milano, IT, Italia.
2. CRUX Engineering BV, Delft, NL, Netherland.
3. Faculty of Civil Engineering and Geosciences, TU Delft, Delft, NL, Netherland.

Abstract
The increasing demand for energy and the need to reduce reliance on fossil fuels in response to climate change have spurred the exploration of renewable energy sources. Energy Geostructures address these issues by providing at the same time mechanical support to overlying structures and/or soil and geothermal energy for space heating and cooling. Energy sheet pile walls are a novel form of Energy Geostructures that utilize sheet pile walls fitted with steel pipe heat exchangers. When used along quays, energy quay walls are known as Energy quay walls (EQWs), offering the advantage of extracting thermal energy from both soil and water. However, the thermal and thermo-mechanical behavior of EQWs is not well understood due to the absence of standardized design methods. Based on a test case installed in Delft (NL), this study focuses on the thermal behavior of EQWs and presents two Finite Element numerical models. The first model reconstructs the initial temperature profile before EQW activation, while the second model enables a detailed analysis of heat exchange processes within the EQW system.
Keywords: Energy Quay wall, Energy Geostructures, Geothermal energy, retaining structures, finite element method.

Introduction

The rising energy demand, primarily reliant on fossil fuels, and concerns about climate change have prompted an intensified exploration of renewable energy sources [1].
The utilization of subsurface resources for heating and cooling purposes has been increasingly embraced through the analysis and design of Energy Geostructures (EGs). These innovative systems not only provide structural support but also harness the subsurface for efficient thermal exchange [2].
Energy sheet pile walls (ESPs) represent a novel form of Energy Geostructures (EGs) that incorporate sheet pile walls fitted with steel pipe heat exchangers. These ESPs offer the advantage of extracting thermal energy from both the soil and water when employed in applications such as canal bank support or port docks [3]. The specific variant employed in open water areas is known as Energy quay walls (EQWs), which are currently being tested at specific locations along canals in the Netherlands [4]. The energy efficiency of EQWs is anticipated to be influenced by several factors, including the undisturbed ground temperature profile, thermal conductivity and thermal capacity of the soil, as well as various operational and construction parameters [5] [6]. However, due to the absence of standardized design methods for EQWs, further research is necessary to comprehensively understand both their thermal and thermo-mechanical behavior [7].
Additionally, there is a limited amount of information available in the existing literature regarding the pre-geothermal activation temperature profile within the soil surrounding EQWs.
Few semi-empirical analytical methods have been developed to estimate the temperature distribution in the soil at various depths [8] [9]. However, it is important to note that these methods typically assume a homogeneous soil half-space, which does not consider the presence of different soil layers or the potential influence of water at one of the EG boundaries. As a result, these existing methods may not adequately account for the complexities associated with the actual subsoil conditions encountered in practice.
In this study, two Finite Element (FE) numerical models were developed based on data gathered from an Energy Quay Wall (EQW) test site located in Delft, Netherlands. The first FE model was created with the objective of reconstructing the initial temperature profile within the specific domain of interest. The second FE model was developed to enable a detailed and accurate 3D analysis of the heat exchange processes occurring within the EQW.

Experimental Set Up

A full-scale experiment of an Energy Quay Wall was conducted in Delft, Netherlands, from October 2020 to July 2022 (Figure 1). The primary objective of this field test was to gain a better understanding of the thermal efficiency of EQW systems.
The EQW test site featured two different types of heat exchangers. The first type, referred to as the "Shallow loop," had a depth of 3 meters and primarily exchanged heat with the canal water, which had an approximate depth of 2 meters. The

second type, known as the "Deep loop", extended to a depth of 15 meters and extracted heat from both soil and water.

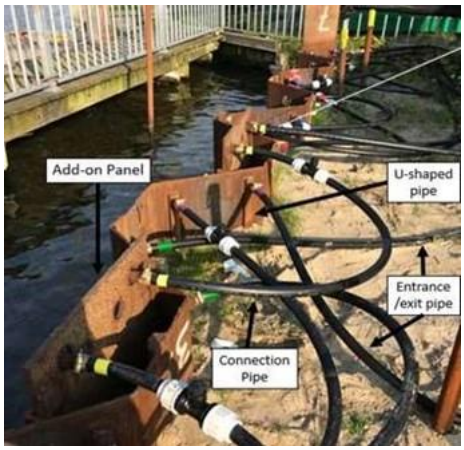

Figure 1. EQW case study installed in Delft (NL)

The loop circuits installed in the EQW system are depicted in Figure 2. These circuits are identified by different colors: purple and green represent the Deep loops, red and blue represent the Shallow loops. Each of these loops comprises a series connection of three U-loops, resulting in a total of 15 U-loops in the EQW system.

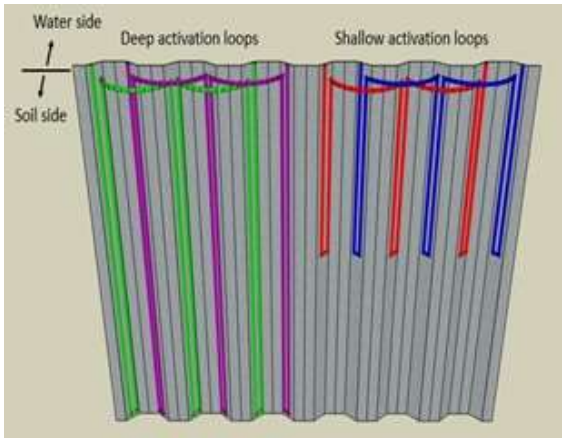

Figure 2. Representation of shallow and deep loops

To monitor and gather data on the EQW system's thermal behaviour and temperature changes within the soil, a comprehensive monitoring system was installed. This system consisted of a total of 59 thermistors, 20 thermowells, and 5 flowmeters. These instruments were employed to measure various parameters, including soil and canal water temperature, heat exchanger fluid temperature, and the flow velocity of both the heat exchanger fluid and the canal water. The EQW system underwent testing with different thermal activation combinations of Deep loops, Shallow loops, and add-on panel loops. These combinations, organized into different phases, were implemented to evaluate the EQW's thermal behaviour and the resulting temperature changes within the surrounding soil [10].

Numerical Model

Two FE numerical models were constructed using the COMSOL Multiphysics software: the “thermal initialization” model to investigate the initial temperature distribution prior to the thermal activation of the EQW [11] and the “Thermal activation” model to conduct a comprehensive analysis of the EQW's thermal performance [12]. The FE models allowed for a thorough examination of the temperature distribution and the heat exchange phenomena within the EQW, providing valuable insights into its thermal performance.

Governing equations

In the EQW-water-soil system, the two primary heat exchange mechanisms are conduction and convection. Convection is the dominant mode of heat transfer between the heat-carrier fluid and the steel pipe walls, whereas conduction is the primary heat exchange process within both the water and soil domains. Although the convection associated with open water was considered, its impact was found to be negligible due to the low velocity of the canal. Radiative heat transfer was deemed negligible and thus not considered in the models. The transient heat diffusion equation governs the conduction process within the system. This equation describes the time-dependent temperature distribution and its evolution over time, accounting for heat transfer through the material.

$$\rho c_p \frac{\partial T}{\partial t} = -\nabla \boldsymbol{q} \quad (1)$$

where q = λ∇T is the heat flux vector described by the Fourier’s law, λ is the thermal conductivity of the medium [W/mK], T is the temperature [K], ρ is the density of the material [kg/m^3], c_p is the specific heat at constant pressure [J/kgK], and t is time [s].

By also considering the convection process, the transient heat equation becomes:

$$\rho c_p \frac{\partial T}{\partial t} + \rho c_p \boldsymbol{u} \cdot \nabla T = 0 \quad (2)$$

where u is the cross-section average fluid velocity along the tangent of the center line of the pipes [m/s].

In order to model the heat exchange within the pipes, a one-dimensional formulation can be utilized by incorporating the momentum conservation and mass conservation equations into the energy balance equation. This allows for a simplified representation of the fluid flow and heat transfer processes:

$$A_p \rho_f c_{pf} \frac{\partial T}{\partial t} + A_p \rho_f c_{pf} \boldsymbol{u} \cdot \nabla T = \nabla A_p \lambda_f \nabla T + f_D \frac{\rho_f A_p}{2 d_h} |u|^3 + q'_{wall} \quad (3)$$

Where A_p is the pipe cross-section area available for flow [m^2], ρ_f is the fluid density [kg/m^3], c_{pf} is the fluid specific heat capacity at constant pressure [J/kgK]. In Eq. (3), the second term on the right-hand side represents the heat dissipated by internal friction within the fluid. This term accounts for the energy loss due to viscous effects and fluid motion within the pipes. Additionally, the term

q'_{wall} represents the radial heat exchange through the pipe walls. It takes into consideration the heat transfer between the fluid and the surrounding pipe material, accounting for any temperature gradients and thermal conductivity of the wall material.

Thermal initialization model

The FE numerical model was developed with the objective of determining the temperature distribution within the soil prior to the thermal activation of the EQW [11]. The model domain has a parallelepipedal shape with dimensions of 26 meters in width, 33 meters in length, and 25 meters in height, as shown in Figure 3.

By placing the boundaries at a significant distance from the EQW, any temperature changes or heat transfer at these boundaries can be minimized. This allows for a more accurate analysis of the heat transfer processes specifically associated with the EQW itself, without interference from external boundary conditions.

The model domain is divided into different soil layers based on their thermal properties. The density, heat capacity, and thermal conductivity of the soil were determined using empirical correlations derived from the results of a cone penetrometer test conducted near the EQW [13]. These empirical results were further validated by referring to existing literature datasets that provided geological characterization of the soil [14]. These bulk thermal properties were assigned to the solid domain elements, while the properties of water and air were taken from the pre-existing material definitions in the software, specifically "Water, liquid" and "Air." The "fluid" node was used to assign these properties to both the air and water layers. Additionally, the "fluid" node includes specifications for the canal velocity component in the y-direction, which is set to 0.02 m/s to represent the real velocity of the canal, known to be relatively constant throughout the year. The wind velocity was also specified as 0.05 m/s to simulate a low wind velocity scenario.

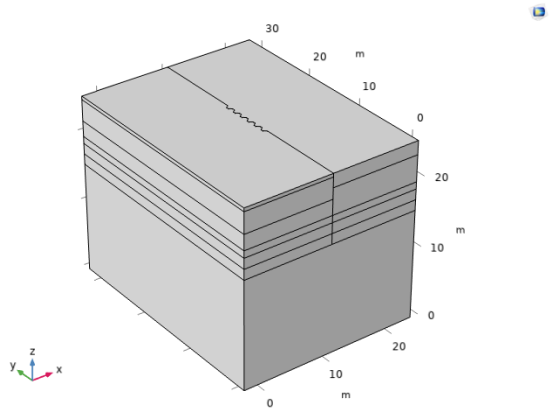

Figure 3. FE numerical model domain implemented in the thermal initialization model.

As regards boundary conditions, the bottom boundary of the model domain was assigned a fixed temperature of 12°C [15], representing the subsurface undisturbed temperature. Thermal insulation was applied to the lateral boundaries to prevent heat transfer through those surfaces. The canal flow was considered by employing inflow and outflow boundary conditions.

To account for the seasonal variations in air and water temperatures, a yearly sinusoidal interpolation was applied based on the temperature data from the previous three years. These sinusoidal curves, representing the temperature variation throughout the year, were repeated ten times to cover a simulation period of ten years. The interpolated air temperature was assigned to all the top boundary surfaces, while the interpolated water temperature was assigned as the inflow temperature for the open water.

The initial temperature distribution within the soil was set equal to the average undisturbed temperature (12°C). This initialization was carried out using the "heat transfer in porous media" module.

The mesh for the numerical simulation was automatically generated using the "Free Tetrahedral" node with finer element sizes calibrated for general physics. This meshing approach ensured an appropriate level of detail for accurate analysis.

To compare the numerical results with the data collected from the monitoring system, the temperature at a total of 59 points within the domain was monitored using the Domain Point Probe node. These points corresponded to the positions of the thermistors in the thermistor strings.

The simulation conducted for this study spanned a period of 10 years from day 0 to day 3650. The timestep was set to 1 day. It should be noted that using smaller mesh elements and a smaller timestep would yield similar results. Thus, these settings were selected to balance computational efficiency and accuracy.

Thermal activation model

In the thermal activation numerical model, several differences are introduced compared to the thermal initialization model. Specifically, the heat exchanger loops that characterize the EQW case study, as depicted in Figure 4, are incorporated into the model. These heat exchanger loops consist of steel U-loops, which extend vertically, and connection pipes made of high-density polyethylene, which have a horizontal orientation and connect the steel U-loops to the heat pump location.

To simulate the heat exchange within these heat exchanger loops, and between the loops and the surrounding solids, the "heat transfer in pipes" module is utilized. This module simplifies the representation of the heat exchanger pipes in a 1D fashion, enabling faster computations.

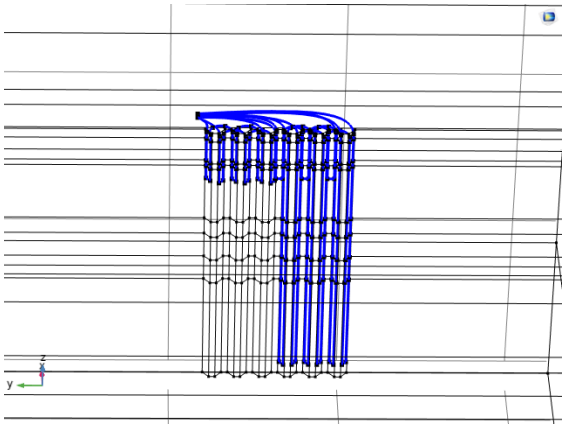

Figure 4. Heat exchanger pipes

In the thermal activation numerical model, several properties and boundary conditions were assigned to accurately represent the EQW system and simulate its thermal behaviour. The key details: (i) The properties of the steel material [16] were assigned to the surface corresponding to the EQW. This includes thermal conductivity, density, and specific heat. (ii) The heat exchanger fluid is a mixture of 80% water and 20% glycol, which reduces the freezing point of the water. The heat capacity and density of the water-glycol mixture were evaluated [16] and assumed constant throughout all simulations. (iii) The thermal conductivity [17] and dynamic viscosity [18] of the heat exchanger fluid were assigned as temperature-dependent functions. These properties change at each timestep based on the temperature of the heat exchanger fluid. (iv) Two different "wall heat transfer" nodes were used to assign the thermal conductivity and wall thickness for the steel pipes and the high-density polyethylene connection pipes. (v) The detected air temperature, water temperature, and temperature at the inlet of each loop were used as boundary conditions for the temperature of the top surfaces, inflow open water temperature, and inlet temperature for each loop, respectively. The detected velocity in each loop was assigned as a time-dependent function. (vi) In addition to the points measuring the temperature in the domain corresponding to each thermistor, five additional probe points were introduced to measure the temperature of the heat exchanger fluid at the outlet of each loop. (vii) The temperature distribution resulting from the thermal initialization model was set as the initial temperature distribution for both the 3D domain and the heat exchanger pipes. (viii) The mesh was automatically generated using the "Free Tetrahedral" node. (ix) The EQW thermal operation was divided into two periods: one with the heat pump active 24 hours a day, and the other with the heat pump active between 10 and 16 hours a day. Two timestep values were considered for each period to simulate them accurately: 1 day for the first period and 0.1 d for the second. (x) The data collected from the monitoring system were taken every 15 minutes, which is much lower than the timestep used in the simulation. To ensure representative data, averages were taken for each timestep to evaluate all the input time-dependent functions. (xi) To ensure that the software uses the exact real input data and achieves a more reliable comparison between the numerical results and the real data, the steps taken by solver were set to "Strict". By enforcing this strict method, the simulation accurately captures the variations in input data from one timestep to the next, providing a more reliable comparison between the simulated and monitored data.

Simulation Results

The results obtained from the simulations were compared to the data collected from the monitoring system to assess the accuracy and reliability of the numerical models.

Thermal initialization

To determine the most accurate temperature profile for the thermal activation model, the numerical simulation results were compared to the measured temperature distribution using the root mean square deviation (RMSE) coefficient. Figure 5 displays the temperature measurements obtained from the DFL sensor string, plotted alongside the corresponding temperature values simulated by the numerical model after 5 years of simulation. The presented figure confirms the consistency between the simulated temperature profile and the actual temperature distribution, thus validating the accuracy of the numerical model.
Figure 6 presents the temperature distribution throughout the domain.

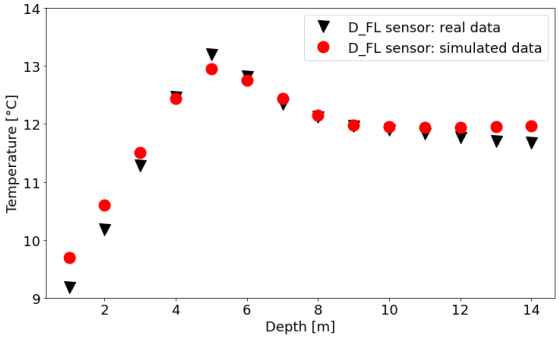

Figure 5. Temperature measured with DFL sensors compare to the ones resulting from the simulation.

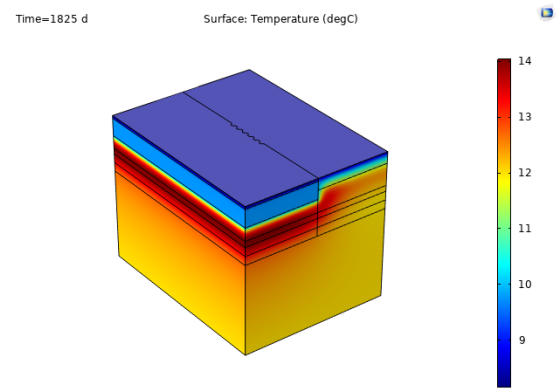

Figure 6. Temperature distribution into soil domain.

Thermal activation

The thermal activation of the EQW system was simulated for the entire 2-year test period. Figure 7 illustrates the comparison between the measured temperature at the inlet of the heat pump and the simulated temperature. Figure 8 shows the comparison between the real temperature variations in the soil and the corresponding simulated values. Figure 9 showcases an example of temperature variation in the soil resulting from the heat exchange between the deep loops and the surrounding soil.
These figures highlight the capability of the numerical model to capture the complex heat exchange processes occurring within the EQW system during its thermal activation phase.

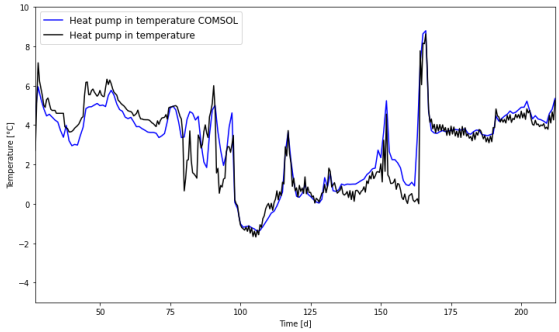

Figure 7. Temperature at the inlet of the heat pump: comparison between the real data and the simulated one. The heat pump is active the whole day.

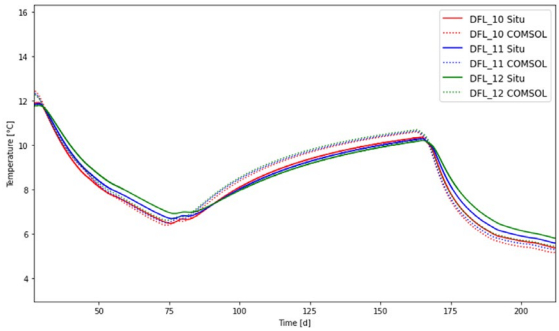

Figure 8. Temperature variation into the soil: comparison between the real one and the simulated one in 3 different points

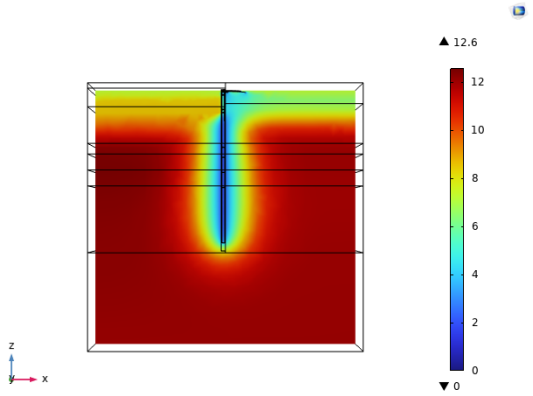

Figure 9. Example of temperature distribution into the soil due to the heat exchange between the deep loops and the surrounding soil.

Discussion

Both the thermal initialization model and the thermal operation model effectively reproduce the behaviour of the EQW system. The thermal initialization model accurately reproduces the temperature distribution in the soil before the thermal activation of the EQW. In Figure 7 and 8, the natural heat storage in the soil after the summer period can be observed, where both air and water temperatures are high. After establishing the initial soil temperature using the thermal initialization model, the thermal operation of the EQW can be simulated. The discrepancy between the actual inlet temperature of the heat pump and the simulated temperature (Figure 8) is minimal. Additionally, the temperature variations in the soil are accurately reproduced by the model. Figure 8 demonstrates two distinct phases: the first and last periods correspond to the activation of the deep loops, where the soil temperature decreases, while the middle period represents the activation of only the shallow loops, leading to an increase in soil temperature due to natural heat conduction within the soil.

Conclusions

The COMSOL Multiphysics numerical model enables the accurate replication of the thermal behaviour of the EQW test case. The initial model focuses on evaluating the temperature distribution in the soil prior to the thermal activation of the EQW, which serves as initial conditions in the subsequent thermal operation numerical model. The thermal operation model successfully reproduces both the temperature at the heat pump's inlet and the temperature variations within the soil.
With the validated model, further analysis is ongoing to identify, for instance, the parameters that have the greatest impact on energy extraction. Additionally, a thermo-mechanical analysis can be performed to assess the thermally induced displacements and stresses within the EQW system.

Acknowledgements

Research funding under the "PON tematica Green – DM 1061/2021" scheme of the Italian Ministry of University and Research, co-funded by CRUX Engineering BV (Delft, NL), is gratefully acknowledged.

References

[1] Baser, T., Mccartney, J. S., & Ozdogan-Dolcek, A.: Thermal energy storage in borehole ar-rays installed in unsaturated soils. Advances in Soil Mechanics and Geotechnical Engineer-ing, 7, 374–390 (2019)

[2] Sanner, B. (2019). Summary of EGC 2019 Country Update Reports on Geothermal Energy in Europe. European Geothermal Congress 2019 Den Haag.

[3] Ziegler, M., Koppmann, D., Peching, R., & Knapp, D. (2019). Energy sheet pile walls – Experimental and numiercal in-vestigation of innovative energy geostructures. XVII European Conference on Soil Mechanics and Geotechnical Engineering.

[4] Haasnoot, J., Vardon, P. J., Pantev, I., Bersan, S., Bloemers, B., & Smeulders, D. (2020). Energy quay walls. E3S Web of Conferences, 205. https://doi.org/10.1051/e3sconf/202020506002

[5] Kürten, S., Mottaghy, D., & Ziegler, M. (2015). A new model for the description of the heat transfer for plane thermo-active geotechnical systems based on thermal resistances. Acta Geotechnica, 10(2), 219–229. https://doi.org/10.1007/s11440-014-0311-6

[6] Kürten, S., Mottaghy, D., & Ziegler, M. (2015). Design of plane energy geostructures based on laboratory tests and nu-merical modelling. Energy and Buildings, 107, 434–444. https://doi.org/10.1016/j.enbuild.2015.08.039

[7] Bourne-Webb, P., Burlon, S., Javed, S., Kürten, S., & Loveridge, F. (2016). Analysis and design methods for energy geo-structures. In Renewable and Sustainable Energy Reviews (Vol. 65, pp. 402–419). Elsevier Ltd.

[8] Brandl, H. (2006). Energy foundations and other thermo-active ground structures. Geotechnique, 56(2), 81–122.

[9] Hillel, D. (1982). Introduction to Soil Physics. In ACADEMIC PRESS. Harcourt Brace Jovanovich Publishers.

[10] de Vries J.P. (2021). Quays rather than boilers: extracting heat from water and soil through energy sheet piles [Master's thesis, TU Delft]. TU Delft Repository.

[11] Gerola, M., Cecinato, F., Haasnoot J., and Vardon, P.J. (2022) Analisi Numerica del Comportamento di una Palancola Energetica. IARG22, Caserta.

[12] Gerola, M., Cecinato, F., Haasnoot J., and Vardon, P.J. (2022). Numerical modelling of Energy Quay Walls to assess their thermal behaviour. Symposium on Energy Geotechnics Accelerating the energy transition 3-5 October 2023, Delft, the Netherlands.

[13] Vardon, P. J., & Peuchen, J. (2021). CPT correlations for thermal properties of soils. Acta Geotechnica, 16(2), 635–646. https://doi.org/10.1007/s11440-020-01027-2

[14] Dalla Santa, G., Galgaro, A., Sassi, R., Cultrera, M., Scotton, P., Mueller, J., Bertermann, D., Mendrinos, D., Pasquali, R., Perego, R., Pera, S., di Sipio, E., Cassiani, G., de Carli, M., & Bernardi, A. (2020). An updated ground thermal prop-erties database for GSHP applications. Geothermics, 85. https://doi.org/10.1016/j.geothermics.2019.101758

[15] Busby, J., Kingdon, A., & Williams, J. (2011). The measured shallow temperature field in Britain. Quarterly Journal of En-gineering Geology and Hydrogeology, 44(3), 373–387. https://doi.org/10.1144/1470-9236/10-049

[16] Laloui, L., Rotta Loria, A. F. (2020).In Analysis and Design of Energy Geostructures. Elsevier. https://doi.org/10.1016/b978-0-12-816223-1.00003-

[17] Cheng, N. S. (2008). "Formula for viscosity of glycerol-water mixture." Industrial and Engineering Chemistry Research, 47, 3285-3288.

[18] Trejo González, J. A., Longinotti, M. P., & Corti, H. R. (2011). The viscosity of glycerol-water mixtures including the supercooled region. Journal of Chemical and Engineering Data, 56(4), 1397–1406. https://doi.org/10.1021/je101164q